

This is a repository copy of *Tidal Forces in Reissner-Nordström Spacetimes*.

White Rose Research Online URL for this paper:

<https://eprints.whiterose.ac.uk/id/eprint/97124/>

Version: Published Version

Article:

Crispino, Luís C. B., Higuchi, Atsushi orcid.org/0000-0002-3703-7021, Oliveira, Leandro A. et al. (1 more author) (2016) Tidal Forces in Reissner-Nordström Spacetimes. European Physical Journal C (Particles and Fields). ISSN: 1434-6052

<https://doi.org/10.1140/epjc/s10052-016-3972-5>

Reuse

This article is distributed under the terms of the Creative Commons Attribution (CC BY) licence. This licence allows you to distribute, remix, tweak, and build upon the work, even commercially, as long as you credit the authors for the original work. More information and the full terms of the licence here:

<https://creativecommons.org/licenses/>

Takedown

If you consider content in White Rose Research Online to be in breach of UK law, please notify us by emailing eprints@whiterose.ac.uk including the URL of the record and the reason for the withdrawal request.

Spectroscopic Quadrupole Moments in $^{96,98}\text{Sr}$: Evidence for Shape Coexistence in Neutron-Rich Strontium Isotopes at $N = 60$

E. Clément,^{1,2,*} M. Zielińska,^{3,4} A. Görgen,⁵ W. Korten,³ S. Péru,⁶ J. Libert,⁶ H. Goutte,³ S. Hilaire,⁶ B. Bastin,¹ C. Bauer,⁷ A. Blazhev,⁸ N. Bree,⁹ B. Bruyneel,⁸ P. A. Butler,¹⁰ J. Butterworth,¹¹ P. Delahaye,^{1,2} A. Dijon,¹ D. T. Doherty,³ A. Ekström,¹² C. Fitzpatrick,¹³ C. Fransen,⁸ G. Georgiev,¹⁴ R. Gernhäuser,¹⁵ H. Hess,⁸ J. Iwanicki,⁴ D. G. Jenkins,¹¹ A. C. Larsen,⁵ J. Ljungvall,¹⁴ R. Lutter,¹⁵ P. Marley,¹¹ K. Moschner,⁸ P. J. Napiorkowski,⁴ J. Pakarinen,² A. Petts,¹⁰ P. Reiter,⁸ T. Renstrøm,⁵ M. Seidlitz,⁸ B. Siebeck,⁸ S. Siem,⁵ C. Sotty,¹⁴ J. Srebrny,⁴ I. Stefanescu,⁹ G. M. Tveten,^{5,2} J. Van de Walle,² M. Vermeulen,¹¹ D. Voulot,² N. Warr,⁸ F. Wenander,²

A. Wiens,⁸ H. De Witte,⁹ and K. Wrzosek-Lipska⁴

¹GANIL, CEA/DSM-CNRS/IN2P3, F-14076 Caen Cedex 05, France

²PH Department, CERN 1211, Geneva 23, Switzerland

³CEA Saclay, IRFU, SPhN, 91191 Gif-sur-Yvette, France

⁴Heavy Ion Laboratory, University of Warsaw, PL-02-093 Warsaw, Poland

⁵Department of Physics, University of Oslo, 0316 Oslo, Norway

⁶CEA, DAM, DIF, F-91297 Arpajon, France

⁷Institut für Kernphysik, Technische Universität Darmstadt, D-50937 Darmstadt, Germany

⁸Institute of Nuclear Physics, University of Cologne, D-50397 Cologne, Germany

⁹Instituut voor Kern-en Stralingsfysica, KU Leuven, Celestijnenlaan 200D, B-3001 Leuven, Belgium

¹⁰Oliver Lodge Laboratory, University of Liverpool, Liverpool L69 7ZE, United Kingdom

¹¹Department of Physics, University of York, YO10 5DD York, United Kingdom

¹²Physics Department, University of Lund, Box 118, SE-221 00 Lund, Sweden

¹³Department of Physics, University of Manchester, M13 9PL Manchester, United Kingdom

¹⁴CSNSM, Université Paris-Sud, CNRS/IN2P3, Université Paris-Saclay, 91405 Orsay, France

¹⁵Fakultät für Physik, Ludwig-Maximilians-Universität München, D-85740 Garching, Germany

(Received 2 September 2015; published 15 January 2016)

Neutron-rich $^{96,98}\text{Sr}$ isotopes have been investigated by safe Coulomb excitation of radioactive beams at the REX-ISOLDE facility. Reduced transition probabilities and spectroscopic quadrupole moments have been extracted from the differential Coulomb excitation cross sections. These results allow, for the first time, the drawing of definite conclusions about the shape coexistence of highly deformed prolate and spherical configurations. In particular, a very small mixing between the coexisting states is observed, contrary to other mass regions where strong mixing is present. Experimental results have been compared to beyond-mean-field calculations using the Gogny D1S interaction in a five-dimensional collective Hamiltonian formalism, which reproduce the shape change at $N = 60$.

DOI: [10.1103/PhysRevLett.116.022701](https://doi.org/10.1103/PhysRevLett.116.022701)

Throughout the nuclear chart, ground-state properties such as nuclear radii and shapes tend to evolve gradually as a function of the nucleon number. However, interactions between nucleons in an effective mean field may cause a sudden rearrangement of the entire nucleus when few protons or neutrons are added, leading to a strong shell closure or a rapid onset of deformation. One of the major challenges in modern nuclear structure studies is to fully understand and describe these abrupt transitions that result from the delicate interplay between macroscopic (i.e.,

liquid droplike) properties and microscopic (i.e., shell structure) effects in nuclear matter.

Dramatic shape changes are often interpreted as a result of an inversion of two distinct quantum configurations of nucleons associated with different nuclear shapes. These structures may coexist at low excitation energy, as observed, for example, in Pb [1], Hg [2], and Kr [3] isotopes. Systematic studies of transition strengths and quadrupole moments in the $^{182-188}\text{Hg}$ [4] and $^{74-76}\text{Kr}$ [3,5] have revealed that both structures tend to strongly mix, which results, for example, in an almost constant excitation energy of the first 2^+ state in $^{182-188}\text{Hg}$. The mixing, reflected both in level energies and transition probabilities, is most prominent when the configurations invert and makes the change of the ground state properties more gradual.

Published by the American Physical Society under the terms of the [Creative Commons Attribution 3.0 License](https://creativecommons.org/licenses/by/3.0/). Further distribution of this work must maintain attribution to the author(s) and the published article's title, journal citation, and DOI.

In a unified description of shape coexistence [6] for nuclei close to proton shell closures, e.g., $Z = 20$ (Ca [7]), 28 (Ni [8]), and 82 (Pb-Hg [9]), spherical configurations corresponding to closed shells compete with deformed configurations resulting from multiparticle multihole excitations above the proton shell closures that interact with neutrons, which fill high- j intruder orbits. The significant gain in nuclear binding energy arising from the pairing and the proton-neutron correlation energy decreases the excitation energy of the corresponding 0_2^+ state in even-even nuclei so that it appears at low excitation energy or even becomes the ground state [6].

The sudden onset of deformation observed for neutron-rich Zr and Sr nuclei at $N = 60$ belongs to the most dramatic shape changes in the nuclear chart. This shape transition is accompanied by the appearance of low-lying 0_2^+ states that, for $N < 60$, can be interpreted as a deformed configuration that becomes the ground state at $N = 60$, while the spherical ground-state configuration of the isotopes with $N < 60$ becomes nonyrast for those with $N \geq 60$. This mass region draws particular attention in the unified description of shape coexistence [6] since the proton number $Z = 40$ is a relatively weak subshell and not a strong proton shell closure, and the spherical-to-deformed transition is sudden. In a conventional picture, the microscopic effects due to a subshell closure would be smeared out by pairing and would have no influence on collective nuclear properties, which is clearly not in agreement with experimental data for this mass region. On the contrary, the irregularity of the two-neutron separation energy and the sudden drop of the excitation energy of the first 2^+ state in Zr and Sr nuclei provides evidence for a dramatic structural change at $N = 60$. The local character of this sudden change was recently established [10,11]. This points to the interaction between specific proton and neutron orbitals as the origin of the phenomenon, making it one of the best examples of a competition between microscopic and macroscopic degrees of freedom in atomic nuclei.

Numerous theoretical studies, using various approaches, have aimed to address shape evolution and coexistence in Sr and Zr isotopes [12–28]. They correctly reproduce the boundaries of the deformed region, but their predictions are mostly limited to what is available experimentally: energy spectra and ground-state properties such as masses and charge radii. While these observables yield information on the configuration of the ground state, properties of coexisting nonyrast structures and the degree of their mixing with the ground-state configuration can only be inferred from transition rates or electromagnetic moments. In this Letter, we report a unique set of spectroscopic data for this mass region, extracted from a multistep Coulomb excitation measurement using postaccelerated radioactive ion beams. The measured transition probabilities between excited states and spectroscopic quadrupole moments in $^{96,98}\text{Sr}$ are used to assess the shape coexistence interpretation,

including a detailed comparison with the first complete beyond-mean-field calculations, for this mass region, that yield electromagnetic properties of both yrast and nonyrast structures on either side of the $N = 60$ shape transition.

The experiment was performed at the REX-ISOLDE facility at CERN. Postaccelerated radioactive beams of ^{96}Sr and ^{98}Sr were delivered with average intensities of 7×10^3 pps at 275 MeV and 6×10^4 pps at 276 MeV, respectively, to the Coulomb excitation setup of the Miniball array [29]. The beam composition after postacceleration was monitored using a ΔE - E detector consisting of a low-pressure ionization chamber and a silicon detector [29], and was determined consistently to be 5% ^{98}Rb , 80% ^{98}Sr , 15% ^{98}Y for mass $A = 98$. Several different targets were used in order to make use of the dependence of the Coulomb excitation cross section on the atomic numbers of collision partners: ^{109}Ag (1.9 mg/cm² thick) and ^{120}Sn (2.0 mg/cm²) in the case of ^{96}Sr , ^{60}Ni (2.1 mg/cm²) and ^{208}Pb (1.5 mg/cm²) for ^{98}Sr . The scattered Sr ions and recoiling target nuclei were detected with an annular silicon strip detector covering an angular range from 20° to 55° in the laboratory frame. Deexcitation γ -ray spectra were sorted in prompt coincidence with scattered particles for scattering angles chosen to ensure a purely electromagnetic process [30]. The γ -ray energy spectrum following Coulomb excitation of the ^{98}Sr beam on the ^{208}Pb target is presented in Fig. 1. The γ -ray energy spectra obtained for the other systems are reported in [31].

For ^{96}Sr , the $2_1^+ \rightarrow 0_1^+$ transition was observed together with excitation of the respective target nuclei and a weak transition corresponding to the 0_2^+ deexcitation. For ^{98}Sr , the rotational ground-state band was populated up to spin 6^+ and 8^+ using ^{60}Ni and ^{208}Pb targets, respectively, and in both cases the decay of the 2_2^+ state was also observed. Several unknown transitions marked with asterisks in Fig. 1 were not in coincidence with any known transitions in ^{98}Sr , and thus, we assume that they belong to the beam

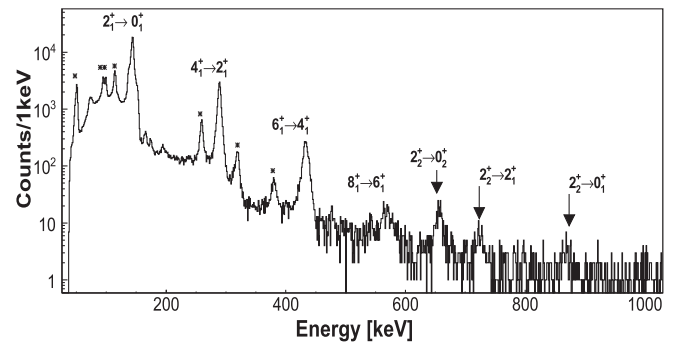


FIG. 1. Total γ -ray energy spectrum following Coulomb excitation of the ^{98}Sr beam impinging on a ^{208}Pb target, Doppler corrected for the projectile. Contaminating transitions, attributed to ^{98}Rb , are marked with asterisks.

contaminant ^{88}Rb , for which no excited states have been reported so far.

The Coulomb excitation analysis was performed using the least squares fitting code GOSIA [32,33]. For ^{96}Sr , where prior to the present experiment the lifetime of the first 2^+ was known only with a large uncertainty (7(4) ps [34]), normalization to the excitation of the ^{120}Sn target was necessary. The influence of the two-step excitation to the 0_2^+ state on the excitation probability of the 2_1^+ state was constrained by including the known lifetime of the 0_2^+ state [34] in the minimization procedure. Following the prescription described in Ref. [33], a χ^2 surface resulting from comparison of experimental and calculated γ -ray intensities in both collision partners, measured for three cuts of scattering angle, as well as spectroscopic data in ^{120}Sn was constructed with respect to the $\langle 2_1^+ || E2 || 0_1^+ \rangle$ and $\langle 2_1^+ || E2 || 2_1^+ \rangle$ matrix elements in ^{96}Sr . The 1σ uncertainties of both matrix elements were obtained by projecting the contour corresponding to $\chi^2_{\min} + 1$ on the respective axes. The transitional matrix element is in agreement with the value calculated from the previously reported lifetime and its precision is significantly improved.

In the case of ^{98}Sr , known lifetimes of the 2_1^+ , 4_1^+ , 8_1^+ , 10_1^+ , and 0_2^+ states [34–40] and the branching ratios for the 0_2^+ and 2_2^+ decays [38,41], including the $E2/E0$ branching ratio [42,43], were used as additional data points in the GOSIA fit. As a result of the minimization process, a set of matrix elements was found that reproduces all experimental γ -ray yields, as well as other spectroscopic data, within 1σ . The resulting $B(E2)$ values and spectroscopic quadrupole moments for both nuclei are presented in Table I and Table II. The associated experimental error bars are coming from the statistical errors on the measured γ -ray intensities.

The spectroscopic quadrupole moments in the ground-state band of ^{98}Sr are large and negative, which is consistent with the enhanced $B(E2)$ values within the ground-state band. This corroborates a rotational character for these states and corresponds to a significant prolate deformation of $\beta_2 \geq +0.3$. In contrast, the diagonal matrix element of the 2_2^+ state in ^{98}Sr is found to be small and consistent with zero within error bars, similar to that of the 2_1^+ state in ^{96}Sr . In addition, the $B(E2; 2_2^+ \rightarrow 0_2^+)$ value in ^{98}Sr is of similar magnitude to the $B(E2; 2_1^+ \rightarrow 0_1^+)$ value in ^{96}Sr , indicating a similarity between these structures. Under the assumption of axial symmetry, the β_2 deformation parameters of the 2_2^+ state in ^{98}Sr and the 2_1^+ state in ^{96}Sr calculated from the measured quadrupole moments are close to 0.1.

The $B(E2)$ values from the 2_2^+ state to the ground-state band are small, suggesting weak mixing between these configurations, in spite of their proximity in energy. This can be further investigated using a two-state mixing model, where the observed physical states $|I_1^+\rangle$ and $|I_2^+\rangle$ are expressed as linear combinations of pure prolate-deformed

TABLE I. Observed γ -ray transitions with their intensities for each system (without efficiency correction) and reduced transition probabilities between low-lying states in $^{96,98}\text{Sr}$. The error bars correspond to 1σ .

^{98}Sr beam	$^{208}\text{Pb}/^{60}\text{Ni}$ target	$B(E2; I_2 \rightarrow I_1) (e^2 b^2)$	
$I_2 \rightarrow I_1$	I_γ	Experiment	5DCH
$2_1^+ \rightarrow 0_1^+$	$1.21(2) \times 10^5 / 5.0(2) \times 10^4$	$0.259^{+0.008}_{-0.008}$	0.1455
$4_1^+ \rightarrow 2_1^+$	$1.80(3) \times 10^4 / 8.06(12) \times 10^3$	$0.345^{+0.022}_{-0.019}$	0.2961
$6_1^+ \rightarrow 4_1^+$	$2.72(7) \times 10^3 / 1.11(5) \times 10^3$	$0.46^{+0.09}_{-0.03}$	0.4037
$8_1^+ \rightarrow 6_1^+$	232(63)/not observed	$0.34^{+0.05}_{-0.04}$	0.4634
$10_1^+ \rightarrow 8_1^+$	From $T_{1/2}$ [39]	$0.34^{+0.08}_{-0.05}$	0.4915
$2_2^+ \rightarrow 0_2^+$	198(21)/128(74)	$0.027^{+0.003}_{-0.003}$	0.0762
$2_2^+ \rightarrow 0_1^+$	From branching ratio [38]	$0.0018^{+0.0003}_{-0.0003}$	0.0002
$0_2^+ \rightarrow 2_1^+$	From $T_{1/2}$ [38,42]	$0.25^{+0.02}_{-0.02}$	0.3243
$2_2^+ \rightarrow 2_1^+$	58(11)/not observed	$0.002^{+0.001}_{-0.001}$	0.0021
$2_2^+ \rightarrow 4_1^+$	From branching ratio [38]	$0.012^{+0.007}_{-0.008}$	0.0521
$B(M1; I_2 \rightarrow I_1) (\mu_N^2)$			
		Experiment	5DCH
$2_1^+ \rightarrow 2_2^+$		$0.0008^{+0.0003}_{-0.0002}$	
^{96}Sr beam	$^{120}\text{Sn}/^{109}\text{Ag}$ target	$B(E2; I_2 \rightarrow I_1) (e^2 b^2)$	
		Experiment	5DCH
$2_1^+ \rightarrow 0_1^+$	660(30)/354(21)	$0.045^{+0.011}_{-0.008}$	0.084

and spherical configurations, $|I_p^+\rangle$ and $|I_s^+\rangle$, respectively. Following the method described in [5], we used the complete set of $E2$ matrix elements in ^{98}Sr , obtained in the present Letter, to determine the mixing amplitudes $\cos^2\theta_0 = 0.82(2)$ and $\cos^2\theta_2 = 0.99(1)$ for the 0_1^+ and 2_1^+ states, which suggests a very low degree of mixing between the two configurations. This is in agreement with the conclusions of Refs. [35,42,44] that used, however, model assumptions to estimate the transition strengths that were not determined experimentally prior to the present Letter. The weak mixing of the coexisting structures in ^{98}Sr is clearly different from what is observed for the neutron-deficient Kr [5] and Hg [4] isotopes, where the mixing of

TABLE II. Spectroscopic quadrupole moments obtained in this Letter in $^{96,98}\text{Sr}$. The error bars correspond to 1σ .

$Q_s (e \text{ fm}^2)$	^{96}Sr		^{98}Sr	
	Experiment	5DCH	Experiment	5DCH
2_1^+	-22^{+33}_{-31}	-5.6	-52^{+24}_{-24}	-60
4_1^+			-187^{+14}_{-25}	-112
6_1^+			-121^{+39}_{-16}	-136
8_1^+			-95^{+74}_{-88}	-149
2_2^+			$+2^{+13}_{-12}$	-28

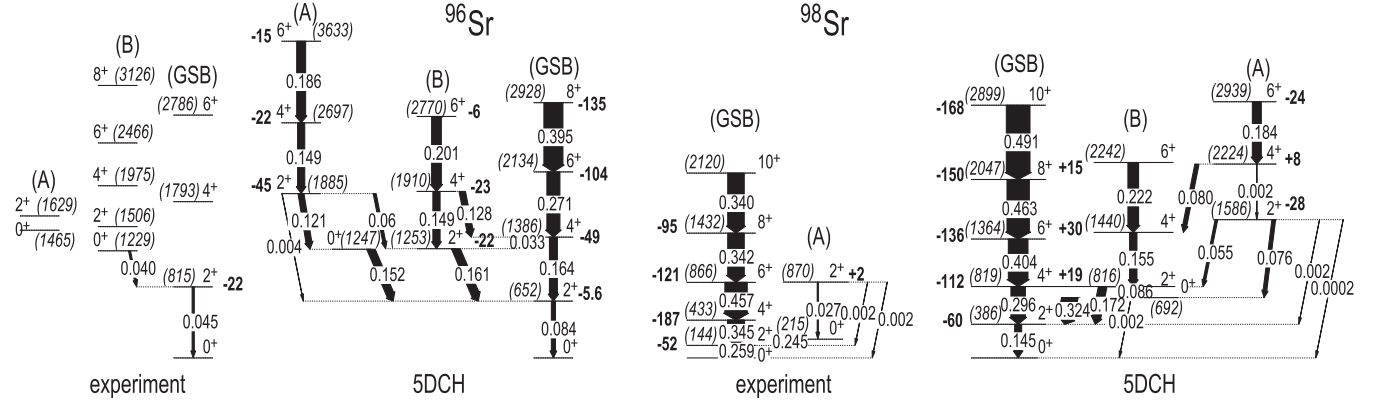


FIG. 2. Comparison between the theoretical and experimental level schemes of ^{96}Sr (left) and ^{98}Sr (right). The excitation energies (in keV) are given in brackets. The widths and labels of the arrows represent the measured and calculated $B(E2)$ in $e^2 b^2$. The measured and calculated spectroscopic quadrupole moments are given in efm^2 next to each state.

the wave functions is large and associated with a smooth shape change. We suggest that this fact is related to the sudden onset of deformation at $N = 60$, and that a larger mixing would give rise to a more gradual transition from a spherical to a deformed ground state in Sr isotopes.

Information on intrinsic quadrupole properties of individual states can be obtained from experimentally determined matrix elements using the quadrupole sum rule approach [30,45]. This method relates $E2$ matrix elements to deformation parameters Q (overall deformation) and δ (deviation from axial symmetry, with $\delta = 0$ for maximum triaxiality) by constructing quadrupole invariants $\langle Q^2 \rangle$ and $\langle Q^3 \cos(3\delta) \rangle$. In ^{98}Sr , an abrupt change in deformation is observed between the ground state [$\langle Q^2 \rangle = 1.30(4) e^2 b^2$] and the low-lying 0_2^+ state [$\langle Q^2 \rangle = 0.38(2) e^2 b^2$]. Since the matrix elements connecting the 0_1^+ state to the $2_{2,3}^+$ states in ^{96}Sr are unknown, the $\langle Q^2 \rangle$ value of $0.22(4) e^2 b^2$ for this nucleus constitutes a lower limit. We note, however, that in the well-studied $N = 58$ isotope ^{100}Mo [43], higher-lying 2^+ states have a minor influence (2%) on the final value of $\langle Q^2 \rangle$. The behavior of the $\langle Q^2 \rangle$ deformation parameters is consistent with what is obtained for the spectroscopic quadrupole moments: the deformation of the ground state in ^{96}Sr and the low-lying 0_2^+ state in ^{98}Sr is similar, supporting the scenario in which these two configurations interchange at $N = 60$. The triaxiality parameters $\langle \cos(3\delta) \rangle$ for $0_{1,2}^+$ states in ^{98}Sr are both equal to $0.46(13)$ and suggest a prolate deformation with a large contribution of the triaxial degree of freedom corresponding to $\bar{\gamma} \approx \bar{\delta} = 1/3 \arccos(\langle \cos(3\delta) \rangle) = 20^\circ$. In view of the similarity between the 0_2^+ state in ^{98}Sr and the 0_1^+ state in ^{96}Sr , one can speculate on a significant contribution of the triaxial degree of freedom for the ^{96}Sr ground state, that could explain the reduction of the 2_1^+ spectroscopic quadrupole moment as compared to the deformation deduced from the $B(E2; 2^+ \rightarrow 0^+)$ value.

We have performed extensive beyond-mean-field calculations using the Gogny D1S interaction in a five-dimensional collective Hamiltonian (5DCH) formalism [46–49] for the ^{96}Sr and ^{98}Sr isotopes in order to interpret the experimental results. The comparison of experimental and theoretical $B(E2)$ and Q_s values are summarized in Fig. 2, Table I, and Table II. The calculated excited states were grouped into band structures (GSB, A, B) as shown in Fig. 2 according to the evolution of their spectroscopic quadrupole moments with spin, the K composition of the wave function, and the reduced transition probabilities between states. The experimental spectroscopic quadrupole moment of the 2_1^+ state in ^{96}Sr , equal to $-22^{+33}_{-31} \text{efm}^2$, is in agreement with the very small calculated value $Q_s = -5.6 \text{efm}^2$. The calculated $B(E2, 2_1^+ \rightarrow 0_1^+)$ and $B(E2, 0_2^+ \rightarrow 2_1^+)$ are significantly higher than the experimental values. The calculations predict, in general, higher collectivity between states than experimentally measured as previously observed for the Kr isotopes with a symmetry-conserving configuration mixing method using the Gogny force [50]. Two excited bands (A, B) are predicted above the low-lying 0_2^+ state. In the excited band (B), the large $B(E2)$ values are not associated with a large axial deformation as indicated by the small spectroscopic quadrupole moments. This band is predicted to have a large contribution from the triaxial degree of freedom with a $K = 0$ component below 50%. It has been shown that the triaxial degree of freedom is a key element in the description of neighboring nuclei [5,50]. The excited band (A) is slightly more deformed with a larger contribution of $K = 0$. Unfortunately, experimental data concerning higher-lying levels in ^{96}Sr are not yet available, which does not allow us to verify these predictions. Similarly, the continuous increase in the quadrupole deformation of the ground-state band, predicted in calculations, awaits experimental verification.

The calculations for ^{98}Sr predict a strongly deformed rotational ground-state band, in agreement with experiment. The calculated moment of inertia is smaller than the experimental one resulting in an underestimation of the transition strengths within the band [48,51,52]. The calculated spectroscopic quadrupole moments are found to be large and negative corresponding to a large prolate deformation, in good agreement with the measurement. As with the Kr case [5], a clear classification of the states and the assignment of nonyrast bands is difficult, due to γ softness and mixing between $K = 0$ and $K = 2$ components. The calculated sequence (A) consisting of the 0_2^+ , 2_3^+ , 4_3^+ , and 6_3^+ states was assigned to the excited (A) band observed experimentally based on the transition strength from the 2_3^+ state to the 0_1^+ and 2_1^+ states: the calculated $B(E2, 2_3^+ \rightarrow 0_1^+)$ and $B(E2, 2_3^+ \rightarrow 2_1^+)$ values are in good agreement with the corresponding transitions from the experimental 2_2^+ state. The calculated energy of the 0_2^+ state is significantly larger than the experimental value. Also, the calculated value of $B(E2, 2_3^+ \rightarrow 0_2^+)$ is three times larger when compared to the experimental value, while the spectroscopic quadrupole moment for the 2_3^+ state ($-28 e\text{fm}^2$) is higher than the experimental value [$+2(13) e\text{fm}^2$]. Nevertheless, the overall agreement justifies the association of the calculated 2_3^+ state with the experimental 2_2^+ state. The first theoretical excited band (B), predicted to be mainly of $K = 2$ character, is most probably calculated too low in excitation energy since it is not observed experimentally. The large calculated $B(E2, 2_2^+ \rightarrow 2_1^+)$ value ($0.172 e^2b^2$) and the relative proximity of the first three 2^+ states suggest a very complex mixing between bands in the theoretical calculation, which could explain the smoother shape transition compared to the experimental results. These discrepancies should be compared with systematic errors of calculated values that could be evaluated as in, for example, [53,54], but this would require developments clearly out of the scope of the present Letter. However, global comparisons of predictions of the present model with experimental data show an overall good agreement especially for deformed nuclei, and the predicted quadrupole properties depend only weakly on the specific Gogny interaction used, as demonstrated in [48,55,56].

In conclusion, the spectroscopic quadrupole moments of low-lying states in ^{96}Sr and ^{98}Sr and reduced transition probabilities between bands were measured for the first time. Spectroscopic quadrupole moments of excited 2^+ states establish a shape coexistence scenario that exists between highly deformed prolate and spherical configurations in ^{98}Sr . A comparison of $B(E2)$ values and the spectroscopic quadrupole moments of the 2_1^+ state in ^{96}Sr and the 2_2^+ state in ^{98}Sr underlines their similarity and establishes the shape inversion at $N = 60$. The interpretation of measured reduced $E2$ matrix elements using a phenomenological two-band mixing model substantiates

the weak mixing between prolate and spherical configurations in the wave functions of the 0^+ states in ^{98}Sr , in spite of their proximity in energy. Our beyond-mean-field calculations support the general picture of coexistence between spherical and deformed configurations which interchange between ^{96}Sr and ^{98}Sr , and properties of individual observed states are in general well reproduced by the present approach, especially in the deformed ^{98}Sr nucleus. Detailed comparisons show, however, that the collectivity in the spherical ^{96}Sr is overestimated by the present model. Extensions of the 5DCH approach such as QRPA or ATDHFB evaluation of vibrational mass parameters could significantly improve the agreement for such a relatively soft and dynamically unstable system. On the other hand, the collectivity of this nucleus might be better reproduced by shell model calculations like those performed for the Zr chain [23], avoiding the restrictions imposed by a pure collective approach. However, a larger valence space using a ^{56}Ni inert core in the shell model calculation would be needed to well describe deformed nuclei beyond $N = 58$ [23], which is currently not possible. Because of the low collectivity of the ground-state band in ^{96}Sr , the deformed structures built on $0_{2,3}^+$ states could not be investigated. Clearly, the measurement of the spectroscopic quadrupole moments beyond the 2_1^+ state in ^{96}Sr and corresponding results in the Zr and Kr isotopes remain a challenge for future RIB facilities.

The work was partially supported by the German BMBF under Contracts No. 06 KY 205, No. 06KY91361, No. 05P12PKFNE, and No. 05P12RDCIB, by the Norwegian Research Council under Contracts No. 180663 and No. 213442, the Research Foundation Flanders (FWO), Belgian Science Office (IUAP), by the U.K. Science & Technology Facilities Council and by the Polish National Science Centre under Contract No. DEC-2013/10/M/ST2/00427. The authors also acknowledge for its support the European Union seventh framework through ENSAR, Contract No. 262010. J. P. acknowledges support of Marie Curie Intra-European Fellowship of the European Community's 7th Framework Programme under Contract No. PIEF-GA-2008-219175.

*clement@ganil.fr

- [1] A. N. Andreyev *et al.*, *Nature (London)* **405**, 430 (2000).
- [2] J. D. Cole *et al.*, *Phys. Rev. Lett.* **37**, 1185 (1976).
- [3] E. Bouchez *et al.*, *Phys. Rev. Lett.* **90**, 082502 (2003).
- [4] N. Bree *et al.*, *Phys. Rev. Lett.* **112**, 162701 (2014).
- [5] E. Clément *et al.*, *Phys. Rev. C* **75**, 054313 (2007).
- [6] K. Heyde and J. L. Wood, *Rev. Mod. Phys.* **83**, 1467 (2011).
- [7] E. Caurier, F. Nowacki, and A. Poves, *Nucl. Phys. A* **742**, 14 (2004).
- [8] D. Pauwels, J. L. Wood, K. Heyde, M. Huyse, R. Julin, and P. Van Duppen, *Phys. Rev. C* **82**, 027304 (2010).
- [9] W. Nazarewicz, *Phys. Lett. B* **305**, 195 (1993).

- [10] S. Naimi *et al.*, *Phys. Rev. Lett.* **105**, 032502 (2010).
- [11] M. Albers *et al.*, *Phys. Rev. Lett.* **108**, 062701 (2012).
- [12] D. Arseniev, A. Sobiczewski, and V.G. Soloviev, *Nucl. Phys.* **A139**, 269 (1969).
- [13] P. Federman and S. Pittel, *Phys. Rev. C* **20**, 820 (1979).
- [14] A. Kumar and M. R. Gunye, *Phys. Rev. C* **32**, 2116 (1985).
- [15] S. Michiaki and A. Akito, *Nucl. Phys.* **A515**, 77 (1990).
- [16] J. Skalski, P.-H. Heenen, and P. Bonche, *Nucl. Phys.* **A559**, 221 (1993).
- [17] A. Baran and W. Höhenberger, *Phys. Rev. C* **52**, 2242 (1995).
- [18] G. Lalazissis and M. M. Sharma, *Nucl. Phys.* **A586**, 201 (1995).
- [19] J. Skalski, S. Mizutori, and W. Nazarewicz, *Nucl. Phys.* **A617**, 282 (1997).
- [20] A. Holt, T. Engeland, M. Hjorth-Jensen, and E. Osnes, *Phys. Rev. C* **61**, 064318 (2000).
- [21] H. Zhang, S. Im, J. Li, W. Zuo, Z. Ma, B. Chen, and W. Scheid, *Eur. Phys. J. A* **30**, 519 (2006).
- [22] T. Rzaca-Urban, K. Sieja, W. Urban, F. Nowacki, J. L. Durell, A. G. Smith, and I. Ahmad, *Phys. Rev. C* **79**, 024319 (2009).
- [23] K. Sieja, F. Nowacki, K. Langanke, and G. Martinez-Pinedo, *Phys. Rev. C* **79**, 064310 (2009).
- [24] R. Rodriguez-Guzman, P. Sarriguren, L. M. Robledo, and S. Perez-Martin, *Phys. Lett. B* **691**, 202 (2010).
- [25] Y.-X. Liu, Y. Sun, X.-H. Zhou, Y.-H. Zhang, S.-Y. Yu, Y.-C. Yang, and H. Jin, *Nucl. Phys.* **A858**, 11 (2011).
- [26] J. Xiang, Z. P. Li, Z. X. Li, J. M. Yao, and J. Meng, *Nucl. Phys.* **A873**, 1 (2012).
- [27] H. Mei, J. Xiang, J. M. Yao, Z. P. Li, and J. Meng, *Phys. Rev. C* **85**, 034321 (2012).
- [28] A. Petrovici, *Phys. Rev. C* **85**, 034337 (2012).
- [29] N. Warr *et al.*, *Eur. Phys. J. A* **49**, 40 (2013).
- [30] D. Cline, *Annu. Rev. Nucl. Part. Sci.* **36**, 683 (1986).
- [31] E. Clément *et al.*, *Eur. Phys. J. Web Conf.* **62**, 01003 (2013).
- [32] T. Czosnyka, D. Cline, and C. Y. Wu, *Bull. Am. Phys. Soc.* **28**, 745 (1983).
- [33] M. Zielińska, L. P. Gaffney, K. Wrzosek-Lipska, E. Clément, T. Grahm, N. Kesteloot, P. Napiorkowski, J. Pakarinen, P. Van Duppen, and N. Warr, [arXiv:1506.04633](https://arxiv.org/abs/1506.04633).
- [34] H. Mach, F. K. Wohn, G. Molnár, K. Sistemich, J. C. Hill, M. Moszyński, R. L. Gill, W. Krips, and D. S. Brenner, *Nucl. Phys.* **A523**, 197 (1991).
- [35] H. Mach, M. Moszyński, R. L. Gill, F. K. Wohn, J. A. Winger, J. C. Hill, G. Molnár, and K. Sistemich, *Phys. Lett. B* **230**, 21 (1989).
- [36] H. Ohm, G. Lhersonneau, K. Sistemich, B. Pfeiffer, and K.-L. Kratz, *Z. Phys. A* **327**, 483 (1987).
- [37] H. Mach, R. L. Gill, and M. Moszyński, *Nucl. Instrum. Methods Phys. Res., Sect. A* **280**, 49 (1989).
- [38] G. Lhersonneau, B. Pfeiffer, R. Capote, J. M. Quesada, H. Gabelmann, and K.-L. Kratz, *Phys. Rev. C* **65**, 024318 (2002).
- [39] A. G. Smith *et al.*, *Phys. Rev. Lett.* **77**, 1711 (1996).
- [40] A. G. Smith, J. L. Durell, W. R. Phillips, W. Urban, P. Sarriguren, and I. Ahmad, *Phys. Rev. C* **86**, 014321 (2012).
- [41] B. Singh and Z. Hu, *Nucl. Data Sheets* **98**, 335 (2003).
- [42] F. Schussler, J. A. Pinston, E. Monnard, A. Moussa, G. Jung, E. Koglin, B. Pfeiffer, R. V. F. Janssens, and J. van Klinken, *Nucl. Phys.* **A339**, 415 (1980).
- [43] K. Wrzosek-Lipska *et al.*, *Phys. Rev. C* **86**, 064305 (2012).
- [44] C. Y. Wu, H. Hua, and D. Cline, *Phys. Rev. C* **68**, 034322 (2003).
- [45] J. Srebrny and D. Cline, *Int. J. Mod. Phys. E* **20**, 422 (2011).
- [46] J. Dechargé and D. Gogny, *Phys. Rev. C* **21**, 1568 (1980).
- [47] J. F. Berger, M. Girod, and D. Gogny, *Comput. Phys. Commun.* **63**, 365 (1991).
- [48] J. P. Delaroche, M. Girod, J. Libert, H. Goutte, S. Hilaire, S. Péru, N. Pillet, and G. F. Bertsch, *Phys. Rev. C* **81**, 014303 (2010).
- [49] J. Libert, M. Girod, and J.-P. Delaroche, *Phys. Rev. C* **60**, 054301 (1999).
- [50] T. R. Rodriguez, *Phys. Rev. C* **90**, 034306 (2014).
- [51] G. F. Bertsch, M. Girod, S. Hilaire, J.-P. Delaroche, H. Goutte, and S. Péru, *Phys. Rev. Lett.* **99**, 032502 (2007).
- [52] S. Péru and M. Martini, *Eur. Phys. J. A* **50**, 88 (2014).
- [53] D. Tarpanov, J. Dobaczewski, J. Toivanen, and B. G. Carlsson, *Phys. Rev. Lett.* **113**, 252501 (2014).
- [54] Y. Gao, J. Dobaczewski, M. Kortelainen, J. Toivanen, and D. Tarpanov, *Phys. Rev. C* **87**, 034324 (2013).
- [55] S. Goriely, S. Hilaire, M. Girod, and S. Péru, *Phys. Rev. Lett.* **102**, 242501 (2009).
- [56] S. Hilaire, M. Girod, and S. Goriely, *J. Korean Phys. Soc.* **59**, 1506 (2011).